DEVELOPMENT AND CHARACTERIZATION OF A DEVICE FOR DELIVERING FUSION FUELS TO THE FOCUS OF A HIGH POWERED LASER

BRENDAN FOLIE

Abstract. A method for depositing nanoscale spheres onto a substrate and subsequently ejecting them is developed. We investigate electrostatic, mechanical, and laser ejection both in theory and in experiment. The electrostatic and mechanical methods proved fruitless, causing us to refine our model of small-scale adhesive forces. Laser cleaning is demonstrated to be successful. Further work is underway to characterize the behavior of particles ejected by a fast laser pulse.

1. Introduction

The interaction of high-intensity ultrafast (sub-100 femtosecond) laser pulses with matter is highly non-linear, and particularly poorly understood when the size of the particles being irradiated is on the order of the wavelength of the laser. Previous simulations and experiments have shown that wavelength-scale spheres experience significant Mie enhancements when pulsed, leading to higher temperature of the emitted electrons and higher energies of the emitted X-rays. The most dramatic effects were observed when the diameter of the spheres d was slightly more than one half the wavelength of the laser λ.[1] However, these studies were limited because the spheres were closely packed and layered on a copper substrate, creating background noise.

The mechanism for this increased hot electron production is believed to be stochastic multi-pass heating. This phenomenon may occur when an ultrafast laser pulse creates a plasma around a sphere and rips out some of the electrons, giving them one ponderomotive kick of energy. The rapidly oscillating electric field then throw the electrons back into the plasma. If the plasma is large enough to delay the electrons but not so large as to completely attenuate them, they will emerge out of phase with the electric field. This allows them to receive another ponderomotive kick, and through repeated kicks acquire large amounts of energy.[2] These high-energy environments make fertile ground for the study of fusion.

In an attempt to better understand this behavior, a device was constructed over the past few years to generate aerosols of micron-scale water droplets. A piezoelectric oscillator was used to create a mist of water droplets in an atomization chamber; varying the frequency of the piezo varies the distribution of droplet sizes. Sucking some of this mist

into a vacuum chamber allows us to address individual droplets with an ultrafast pulse. The extremely high energies present make fertile ground for fusion research, and by using deuterated water, the group was able to observe 2000 fusion neutrons per incident Joule of laser energy.[3] The downside is that the droplets come in a distribution of sizes instead of being monodisperse, and that they are surrounded by a carrier gas from the atomization chamber.

With this in mind, the goal of the group this summer was to develop and characterize a device capable of reliably delivering a cloud of monodisperse spheres across a gap in vacuum. Such a device would be directly applicable to the study of both stochastic multi-pass heating and laser driven fusion.

2. A New Vacuum System

The ultrafast laser systems required to probe for stochastic multi-pass heating must be focused down in high vacuum, therefore any ejection system we design must work in high vacuum as well. Last year the group designed and ordered a large (89 Liter) stainless steel vacuum chamber for this purpose. It includes viewing ports, voltage feedthroughs, vacuum pump feedthroughs, vacuum gauge ports, and high quality sight ports to let in or out a laser beam.

We also own a Welch 1402 Roughing pump, which is capable of pumping the chamber down to 0.2 Torr after a few minutes, and 0.05 Torr after an hour. This is not only a poor approximation of the high vacuum surrounding an ultrafast pulse, but it also leads to some unexpected problems. Particularly, if an ejection method is to involve high voltage, going to rough vacuum makes arcing a serious problem.

Consider two electrodes separated by a gap d and potential difference V_c. At atmospheric pressure, electrons accelerated off of one electrode experience many collisions with free gas molecules on their path to the other electrode, never acquiring enough kinetic energy to start a breakdown avalanche. As the pressure drops and the mean free path of the electrons increases, they acquire more energy and arcing becomes more likely. However, past a certain point the gas is so thin that most electrons cross without interacting with a single gas molecule, and arcing never occurs. *Paschen's Law* states that the arcing voltage at pressure p is:

$$V_c = \frac{apd}{\ln(pd) + b} \tag{1}$$

Where $b = 12.8$ and a is a parameter that depends on the gas. For air, $a = 43.6 \cdot 10^6$ V/atm $\cdot$ m. Treating $p \cdot d$ as one variable, the absolute minimum breakdown voltage can be found by setting $\frac{\partial V}{\partial (pd)} = 0$. The resulting relation is

$$pd = e^{1-b} = 7.5 \cdot 10^{-6} \text{ m} \cdot \text{atm} \tag{2}$$

If we let the chamber pump down to 0.2 Torr, this minimum breakdown voltage will occur across a gap of 2.85 cm, which is exactly the size scale between the positive plate and the (all grounded) scaffolding of the negative plate. If we are patient and let the chamber pump down to 0.05 Torr we have improved the minimum distance to 11.4 cm, but this is still the order of distance between the positive plate and the grounded walls of the chamber. This minimum arcing voltage occurs at 327 V, which is not particularly high.[4]

Clearly, we need a better pump. Note that Paschen's law gives a negative breakdown voltage when $\ln(pd) + b < 0$, indicating arcing is impossible. Therefore, we can obviate the problem by restricting ourselves to a regime where $pd < e^{-b} = 2.76 * 10^{-6}$ m $\cdot$ atm. Given the longest distance between two points in our chamber is less than 1 m, we will be absolutely safe if we can get the pressure below 2 mTorr.

At the beginning of the summer, I helped design and purchase a high vacuum pump system. We decided to make the centerpiece a turbomolecular pump, because these pumps are compact, relatively maintenance-free, require few accessories, and can be bought refurbished for cheap. Turbo pumps utilize a series of bladed turbine rotors, with each blade angled away from the vacuum chamber. The blades direct individual gas molecules out of the chamber and back towards the roughing pump.[5]

We ended up purchasing a refurbished Varian Turbo-V200, so named because it is capable of a nominal pumping speed of 200 liters/second. It is theoretically capable of holding a pressure of 10^{-9} Torr if the chamber is a priori baked at a high temperature to remove hydrocarbons, and 10^{-6} Torr without baking. It requires a foreline pressure of .75 Torr before it can be switched on, but our roughing pump can achieve this in a few minutes. We also purchased a hot cathode Bayard-Alpert gauge capable of measuring pressure as low as $2 \cdot 10^{-9}$ Torr.

When the turbo pump is turned on, the pressure very rapidly falls to around $4 \cdot 10^{-3}$ Torr. It requires 15 minutes to cross the arcing threshold as predicted by Paschen's law, and after an hour is around $6 \cdot 10^{-4}$ Torr. If left on overnight, it is able to achieve a steady pressure of $5.7 \cdot 10^{-5}$ Torr. Having a fully function vacuum system gives us increased flexibility in designing a sphere ejection system, and could also prove useful for any number of projects in the future.

3. Electrostatic Ejection Model

Our first attempts at ejection utilized electrostatic forces. We deposited the spheres on a conducting substrate, placed it near another conducting material, and put a high potential difference between the two. This may force charge onto the substrate and spheres, creating a large repulsive force between them. I created a model of electrostatic ejection,

to determine its viability.

We decided to use stainless steel needles as substrates, because they come to a sharp tip, and sharp corners tend to enhance electric fields. Due to the strange geometry, the problem of finding the electric field along a path between the two needles is non-trivial. We then need to model the contact forces on a sphere, and compare them to the electric pull-off force. Finally, we can use our knowledge of the electric field to predict the spheres' flight between the needles. Knowing how the distribution of spheres moves would be a good first step towards intercepting them with an ultrafast laser pulse.

We have two needles with their tips facing each other, separated by some gap distance L. We know that one is held at voltage V_0, and the other is at ground. We also know the walls of the vacuum chamber (which are about 30 cm away) are held at ground. Modeling the entire vacuum chamber would be computationally very expensive and yield little useful information, so we need to place an artificial boundary around the needles and declare it to be "at ground." The smaller we make our space the less computing needs to be done, but the less exact the solution will be.

To model the needles themselves, I considered the Scanning Electron Microscope (SEM) pictures shown in figure 1

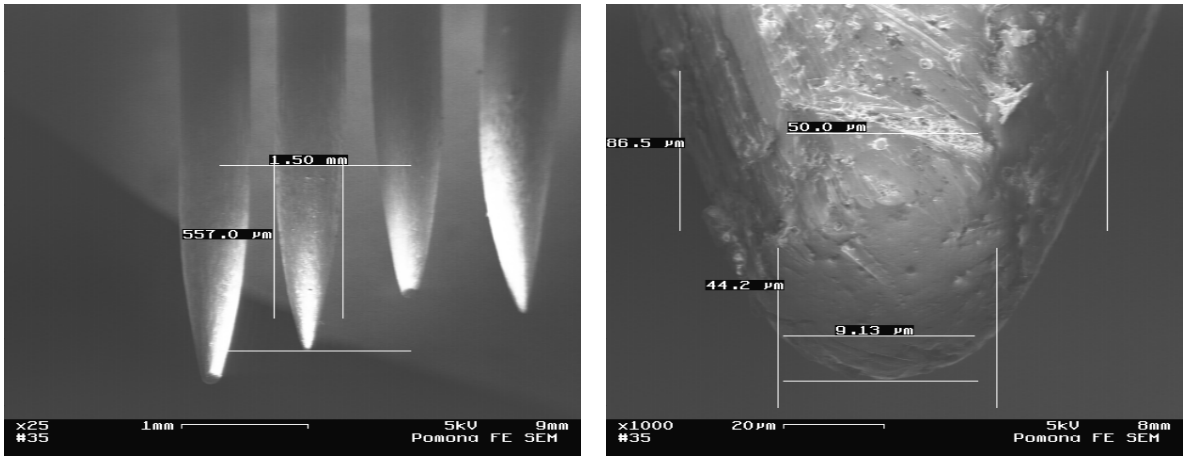

FIGURE 1. Two SEM images of stainless steel sewing needles, with measurements included. The needles are angled at 45 degrees down, so all vertical measurements need to be multiplied by a factor of $\sqrt{2}$. Based on these images, I decided to model the needles as truncated cylindrical cones.

Now that we have the two needles, we can construct a domain where the voltage is known entirely on the boundary (V_0 on one needle, 0 on the other needle and the border). From

electrostatics, we know the voltage in a charge free region (such as between the needles) obeys Laplace's equation:

$$\nabla^2 V = 0 \tag{3}$$

With the voltage on the boundary specified, this equation is guaranteed to have a unique solution on the interior. To approximate the solution, I used the *relaxation method*. It stems from the observation that solutions to Laplace's equation are "as flat as possible," and that the value at each point is the average of the values around it. Therefore by discretizing the domain and iteratively setting each point to be the average of its four neighbors, we approach the exact solution. Plugging in the size and shape of our needles, the results of this simulation are in figure 2.

With a complete description of the electric field, the final thing to model is the forces on an individual sphere. Before being pulled off, it is subject to both adhesive and electrostatic forces. The electrostatic force is equal to the product of electric field and charge. If the needle is at voltage V_0, the sphere is as well (how valid this approximation is depends on the sphere used, and will be discussed shortly). This manifests itself as a charge q distributed evenly on the surface, given by

$$q = 4\pi\epsilon_0 R V_0 \tag{4}$$

The electric field is determined from the simulation, but for the sake of clarity note that it will be on the order of V_0/L (this is the exact solution for the electric field between two infinite parallel plates separated by L and at potential difference V_0). Therefore I will write the electric field as $E = \dfrac{cV_0}{L}$ Where c is some constant that depends on the geometry. For this particular needle size, I found c to be just under 4 (a significant enhancement). Therefore, the force pulling a sphere off the needle is:

$$F = \frac{4\pi c\epsilon_0 R V_0^2}{L} \tag{5}$$

Plugging in a reasonable separation of $L = 1.0$ mm and a maximum voltage $V_0 = 5$ kV, this force is approximately $2.8R$. The fact that the force is linear in R is promising- it means it will not drop off too quickly as we move to smaller spheres.

On the other hand, we have adhesion forces. For this type of particle the only forces are electrical, capillary, and Van der Waals. The high voltages we apply when pulsing completely overpower any stray charge initially on the spheres, so electrical forces are accounted for. Capillary forces occur when an attractive meniscus forms between the sphere and substrate, but because we work at medium to high vacuum, we initially believed capillary forces would be negligible. This leaves Van der Waals, a well understood force.

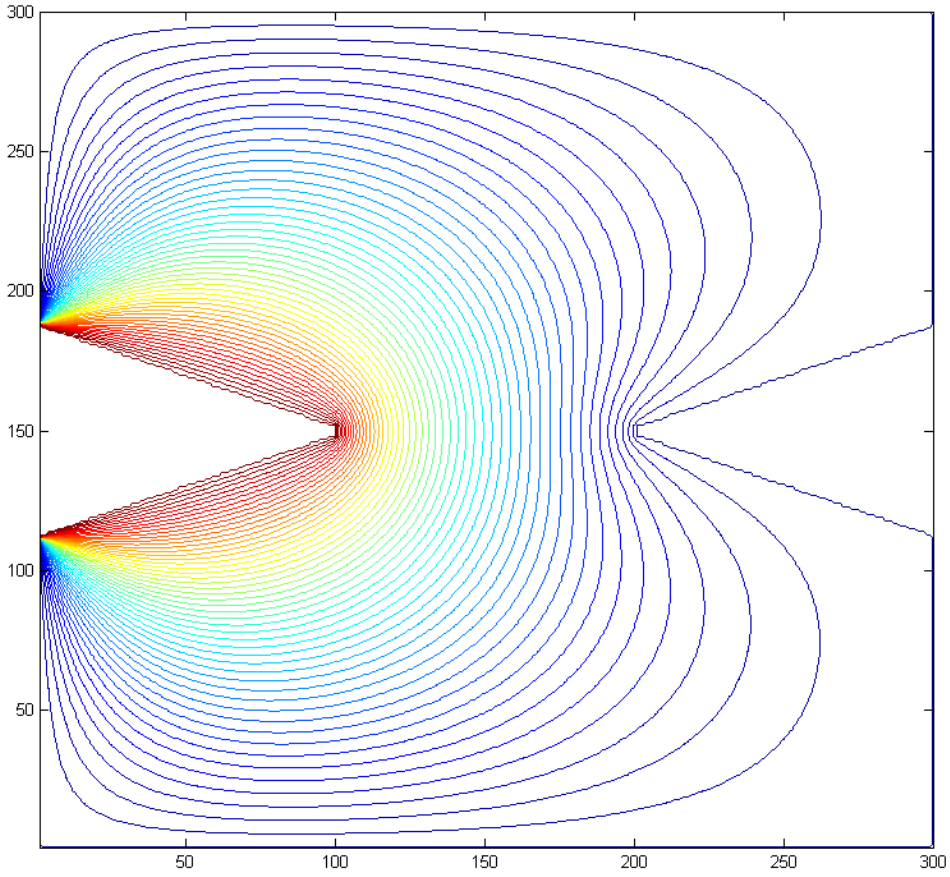

FIGURE 2. A contour plot of the voltage between two needles with an applied potential difference. Each curve is a line of equipotential, going from 0 (black) to V_0 (dark red) in 50 evenly spaced steps. The field lines are more tightly packed around the needle tips, indicating a stronger electric field.

The Van der Waals force between a perfect sphere and an infinite plane is an exactly solved problem, given by:

$$F_{vdW}^{sph} = \frac{A_{ab}R}{2^{10/3}z_0^2} \tag{6}$$

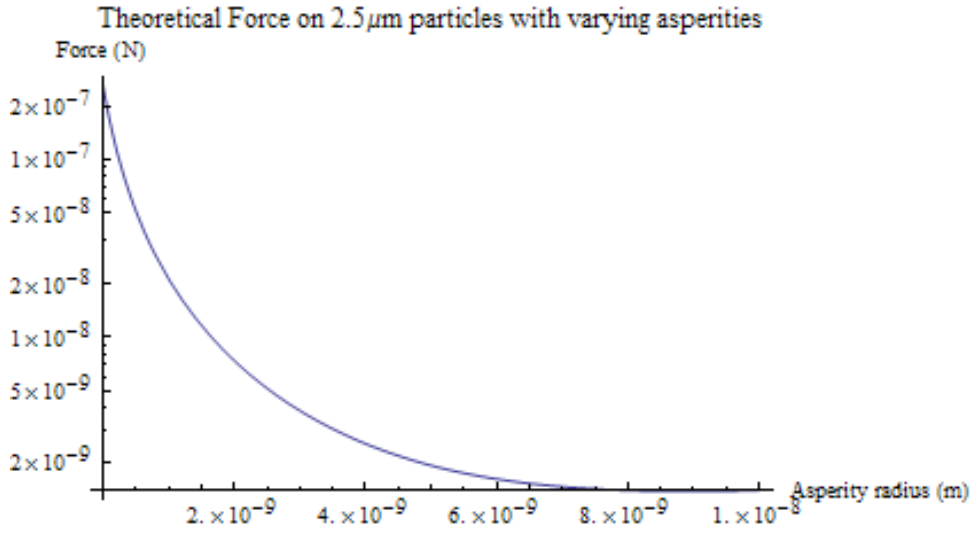

FIGURE 3. A plot of the Van der Waals adhesion force (in Newtons) as experienced by a $R = 2.5$ μm polystyrene particle with a semi-circular asperity of radius r_{asp}. r_{asp} varies from 0 to 20nm along the x-axis. The Van der Waals force is a result of short-range attraction between fluctuating dipoles, therefore it depends very strongly on the separation between the particle and substrate. Takeuchi's prediction is matched for a theoretical asperity of size 0.6nm. The asperities on our spheres come mainly from the polystyrene chain terminating carboxyl groups, which should be on the order of 1nm.

A_{ab} is known as the Hamaker constant; it is typically on the order of 10^{-19} J for interactions across a vacuum. z_0 is the separation between the two bodies, generally taken to be 0.4 nm.[6] Plugging in these values, the Van der Waals force is a measly $0.06R$. Of course the spheres are not perfect- the polystyrene chain-terminated carboxylate groups jut out as asperities. Modeling an asperity as a half-sphere of radius r_{asp}, the Van der Waals force due to the asperity F_{vdW}^{asp} can also be solved for.[6] For my model, I considered a distribution of spheres with randomly generated asperities, and took the total contact force to be $F_{vdW}^{asp} + F_{vdW}^{sph}$.

Takeuchi has done extensive studies on the adhesion forces affecting toner particles. The experiment he did that most nearly mimics our setup was on lightly charged particles with $R = 2.5$ μm. He found the average adhesion force is $4 \cdot 10^{-8}$ N.[7] For comparison, figure 3 shows the theoretical adhesion force as given by (6) plus the force due to some asperity. Note that Takeuchi's results are predicted for a particle with a very modest asperity, giving me confidence in the model.

The behavior of any individual sphere is now completely determined by solving Newton's law, a second order differential equation. I had MatLab numerically approximate the behavior of spheres of radius $R = 250$ nm. The results are shown in figure 4. The spheres

are all removed at voltages far below 5 kV, and fly across the gap very rapidly. They also remain almost entirely with 0.5 mm of each other. These results suggest that electrostatic ejection is worth trying.

4. Ejection Tests

The results of the model were promising, but the proof is in the experiment. We began with polystyrene spheres, available from Thermo Scientific, because of their uniformity and monodispersity. The coefficient of variation in diameter is less than 2%, and they are available in sizes as small as 20 nm. Additionally they can be purchased deuterated, making them possible targets for fusion experiments. However polystyrene is an insulator, and a quick calculation shows it has an appreciable charging time. Therefore it is not surprising that when we deposited them onto a needle and pulsed to high voltage, the spheres were unaffected.

In order to get the charge onto the spheres we employed a sputter coater, a machine that coats the sample in a thin layer of gold. One is typically employed to give a macroscopic object a conducting layer, making it possible to image in an SEM. We tried depositing spheres on a substrate and then sputter coating the whole thing, in the hope that a conducting bridge would be formed between the substrate and a shell of gold around each sphere. A calculation of the resistance shows that even for a 1 nm shell of gold, the charging time is on the order of femtoseconds. This means the voltage on the sphere would be essentially equal to that on the substrate, and equation (4) is valid. Of course, this assumes a gold shell really did form all around the particles

Over the course of several weeks we conducted trials with polystyrene, sputter coated polystyrene, and pure gold spheres. The gold particles came from Nanopartz. They are much less uniform than the polystyrene, and the largest size them come in is 200 nm diameter, however they are known to be completely conducting. For the substrate we used needles, slides coated in Indium Tin Oxide (ITO- a conducting layer), glass slides that had been sputter coated, and silicon slides. The silicon is not as good a conductor as ITO or needles, but it images very well under an SEM. To deposit the spheres we diluted the basic solutions in ethanol (experimenting with different ratios), and dropped this new solution directly onto the substrate. We also experimented with different iterations of dropping, sputter coating, and transferring spheres in order to get a layer of gold completely encapsulating each particle.

Not once did we observe any evidence of sphere ejection.

5. Mechanical ejection

Concurrent with electrostatic ejection, we also attempted to remove the spheres by delivering a large, mechanical shock. The advantage of mechanical methods is that they

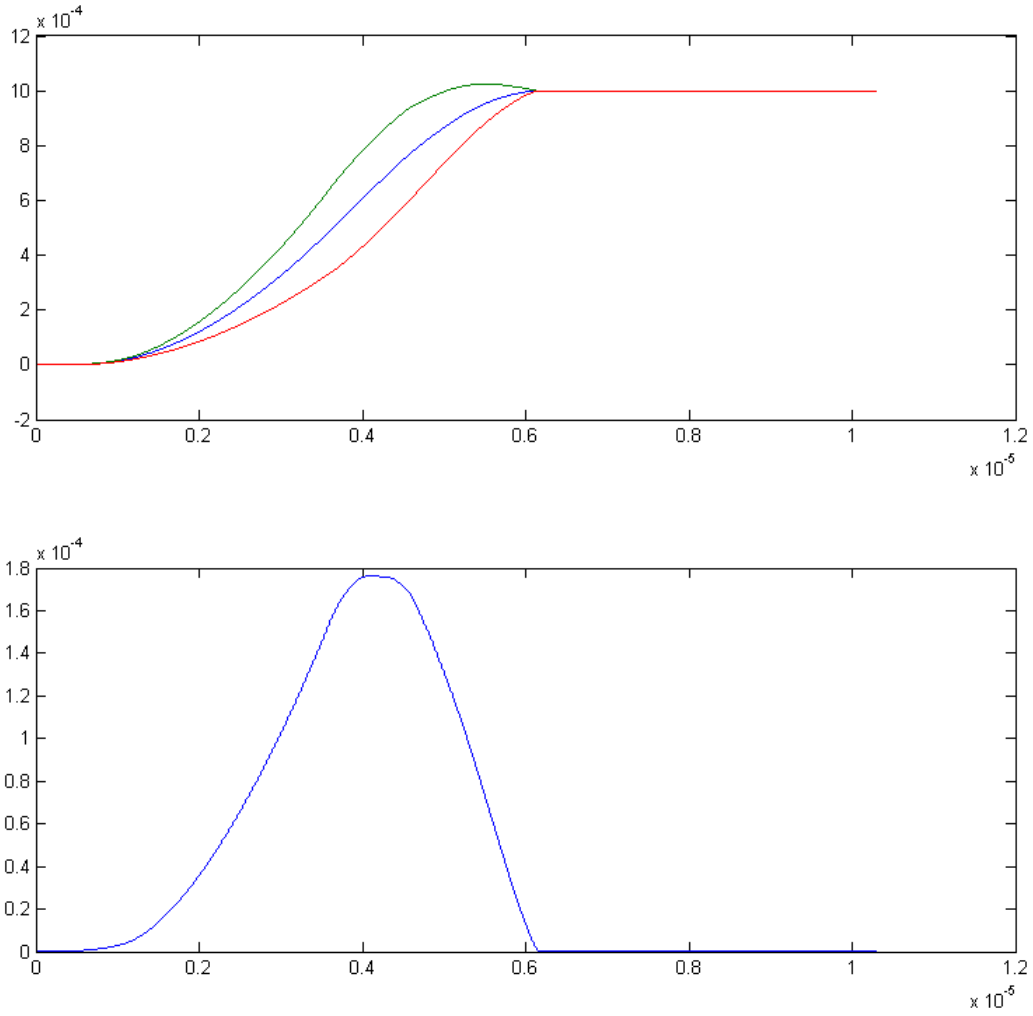

FIGURE 4. Two plots representing the behavior of electrostatically ejected spheres. The spheres have radius $R = 250$ nm, and the pulse rises linearly from 0 to 5 kV over a timespan of 10 μs. The x-axis on both plots is time (in seconds) and the y-axis is a length (in meters). The top plot depicts the center of mass of the spheres in blue. The red and green lines provide an envelope of plus or minus one standard deviation. The bottom plot just displays the standard deviation of the positions of all the spheres. We see the first spheres are ejected after only 1 μs (when the voltage is around 500 V), by 4 μs they are concentrated in the middle, and after 6 μs every sphere is across the gap. For smaller spheres, the timescale would be even shorter

produce constant acceleration. By Newton's law the applied force is equal to mass times acceleration. Since the mass of a sphere is proportional to R^3, the force is as well. This makes mechanical methods useless for very small particles, but viable for larger ones.

Specifically, we attempted to accelerate the spheres using a piezoelectric disc. A piezo is formed by taking a special crystal, heating it to high temperatures, applying a strong external field, and maintaining the field as the crystal cools. This causes all the internal dipoles to lock into one orientation, and the crystal henceforth flexes under an applied electric field. If the applied voltage is an alternating current with angular frequency ω, the crystal also vibrates with frequency ω.[8] The maximum acceleration on the face of the disc is therefore $a = A\omega^2$, where A is the amplitude of the oscillation. If ρ is the density of the spheres, the overall maximum force is therefore

$$F_p = A\omega^2 \frac{4}{3}\pi R^3 \rho \tag{7}$$

We used discs from American Piezo with resonant frequency $\omega \approx 2\pi \cdot 1.6 \cdot 10^6$Hz. Off resonance the amplitude of oscillation is on the order of 100 nm, but at resonance it can be as much as 10 μm at the center of the disc. For polystyrene spheres, equation (7) simplifies to

$$F_p \approx 4.3 \cdot 10^{12} \cdot R^3 \tag{8}$$

For a 5 μm diameter sphere, this mechanical force bests the electrostatic ejection by a factor of 10. Additionally, while the validity of the electrostatic model depends on sputter coating and perfect pulser performance, the mechanical method is simple and requires no great leaps of faith.

Once again we failed to see any evidence of particle ejection, even for the laregst spheres.

6. Dry deposition

At this point we were very worried, and figured there must be some large flaw in our model of the contact forces. The Van der Waals and electrical forces are well understood and our predictions matched with the results of Takeuchi, but he was using dry toner particles. We had always assumed the capillary forces were negligible in vacuum, but decided to reconsider this assumption.

It is known that when a particle from solution dries on a surface or a dry particle is deposited in a humid environment, a small meniscus of water forms between the substrate and the particle. This meniscus rises from the substrate to meet the particle at some angle θ from the vertical. It has a radius of curvature r, where r is negative. See figure 5 for a diagram. A meniscus exerts an attractive force on the sphere, due primarily to the surface

tension of the liquid γ. The most interesting result is that as the meniscus disappears ($\theta \to 0$) the force does *not* go to 0. Instead, it approaches a constant.[9]

$$F_m \to 4\pi\gamma R \tag{9}$$

Plugging in the surface tension for water at room temperature, this force is approximately $F_m = 0.9R$. It is linear in R, and not insignificant when compared to the other forces discussed so far. This theory only breaks down when the meniscus becomes so small that the liquid can no longer be approximated as a continuum, and individual molecules must be discussed.

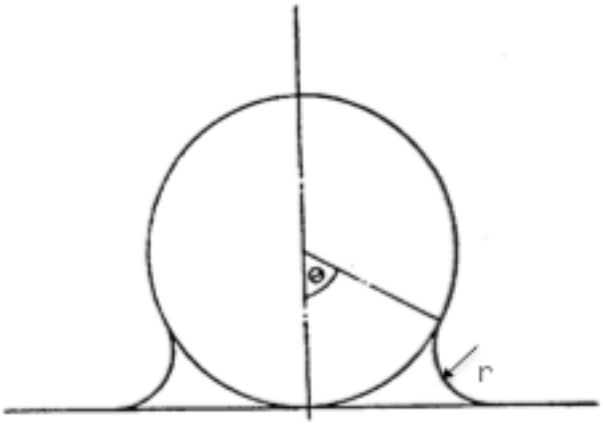

FIGURE 5. A profile view of a sphere of radius R sitting on a plane. A small meniscus of radius r (where r is negative because the curvature is concave) rises up to meet the sphere at an angle of θ from the vertical. This figure is adapted from [10].

The vapor pressure of water is generally 23 Torr, so at high vacuum we would expect the meniscus to evaporate entirely. However, the Kelvin equation predicts that the vapor pressure changes as a liquid interface bends into a radius of curvature r. If p_∞ is the nominal vapor pressure, T is the temperature, R_g is the gas constant, and V_m is the molar volume of the liquid, then the actual vapor pressure p is given by the Kelvin equation.[10]

$$\log \frac{p}{p_\infty} = \frac{2\gamma V_m}{r R_g T} \tag{10}$$

This equation predicts that a meniscus (which has a negative radius of curvature) will result in a decreased vapor pressure. If the meniscus is of radius 0.34 nm, the vapor pressure is drastically lowered to 1 Torr. To bring the vapor pressure down to 10^{-4} Torr (around the level of the vacuum we create) requires a meniscus of radius 0.087 nm. At first glance we appear to be safe. This radius is on the order of an individual water molecule, meaning equation (9) has broken down and there is no capillary force. However, two published results imply that this is not the case. In a thorough study of fine particle adhesion, Ranade found that baking a sample at high temperatures for upwards of 24 hours did not reduce the adhesion forces at all.[11] More to the point, Hecht has the following to say about particles in solution.[13]

> "It seems that once wet particles are allowed to dry on a surface, they are almost impossible to remove. Apparently the small liquid bridge dries into a crystalline structure with such strong adhesion to both the particle and the surface that only immersion back into the liquid can remove the particle."

Our spheres come with a small amount of surfactant to prevent clumping, and other impurities are bound to get into the solution. These results imply that water crystallizes around each impurity, forming countless tiny adhesive bridges that cannot be evaporated away. Ejecting the spheres as they are currently deposited may therefore be impossible.

The only way to salvage electrostatic and mechanical ejection methods was to come up with a deposition method involving absolutely no liquid, however the spheres are initially in solution. Therefore we need to somehow dry them out in transit to the collection slide. Luckily, a former student's work involved a very similar process.

When a piezo is placed at the bottom of a large water bath and driven, it is known that micron-scale droplets are pinched off from the bulk of the fluid. The diameter of these droplets is related to the driving frequency of the piezo as $\omega^{-2/3}$. Using our 1.6 MHz piezos in room temperature water, the droplets produced are around 1.5 μm. Ian Wright, a former student with my advisor, did this with a small amount of chitosan mixed into the water. He then used a pump to force the atomized droplets through a copper pipe that was heated to high temperatures, and finally through a column of desiccating crystals. This evaporates the water, leaving a small ball of chitosan. He placed a collecting silicon slide at the end, and found a very sparse layer of chitosan nanospheres had been deposited.[12]

We adapted this method by dropping some sphere solution in the water. Hopefully some drops will form with nanoparticles at the center, and the water will evaporate as the particles travel through the heating pipe. In addition to the heating pipe, we also tried to evaporate the water using vacuum. We connected the piezo atomization chamber to a valve into the vacuum chamber, and pumped the chamber down to rough vacuum. The valve was opened briefly to suck up the microdroplets, reminiscent of the work done in [3]. The water should evaporate as the droplets travel through vacuum (vapor pressure changes as given by equation (10) are not detrimental for a positively curved drop of water), and we placed a collection slide by the pump outlet to catch the now bare droplets.

Over multiple trials, we discovered that ITO slides get very dirty on the nanometer scale, and are difficult to clean. Silicon, however, can be easily cleaned in an aqua regia bath and images very nicely. The atomization process created droplets with encapsulated spheres, and the water evaporated, but the moving air pushed everything around the edges of the slide. As a result, we saw a few isolated clumps on the edge of the substrate, each with thousands of spheres. This held true for both polystyrene and gold particles. In order to better streamline the flow of air, we tried using a metal mesh for a substrate. No spheres

were observed to adhere, even when the mesh was held at positive voltage.

With dry deposition not producing a nice monolayer and time running short we decided to move onto laser cleaning. However, dry deposition may still be successful if we use a mesh with holes that are only slightly larger than the spheres.

7. Laser Cleaning

In the semiconductor industry, the standard method of cleaning 100 nm-scale contaminant particles from surfaces (generally silicon) is to use a fast laser pulse.[14][15][16][17][18][19] The beam is focused down onto the substrate to be cleaned, causing large amounts of energy to be deposited into the substrate very rapidly. This energy takes the form of heat, causing the substrate to expand and imparting an acceleration to the particles. In addition to this purely mechanical force, the light is known to be strongly enhanced around each wavelength-scale particle, which may cause an explosive boiling of any meniscus present. Not only does laser cleaning remove our meniscus problem, but this boiling may even provide an additional detachment force.

In studying laser cleaning for the semiconductor industry, not damaging the substrate is of paramount importance. Therefore, many studies utilize hundreds or thousands of shots in quick succession, each with a low energy. On the other hand they have no interest in observing the removed particles, so a common technique is to douse the substrate in a thin (1 μm) layer of water immediately before pulsing. This is known as *steam cleaning*, as opposed to what we will do which is *dry cleaning*. It enhances the explosive boiling mentioned above, and may also negate the crystallization as discussed by Hecht. We need to remove most of the particles with one shot and observe their path, yet have no qualms about damaging the substrate.

Experiments have been done on polystyrene, silica, gold, and Al_2O_3 particles. All could be removed by steam cleaning if multiple shots were allowed. The minimum laser fluence (energy per unit area) required varied from the order of 100 mJ/cm^2 to several Joules per square centimeter. Dry cleaning has been found to be generally viable, but less efficient. There is an exception- Zapka & Ziemlich found that 0.2 μm gold particles could not be ejected, and instead started to melt around 5 J/cm^2. The effected removal area tended to be at most 1 mm^2. Finally, one group did a study of the paths of the ejected particles.[20] They found the dry cleaned particles are ejected in a Gaussian distribution, with most going out within $\pm 20^\circ$ of the incident beam. They also found that smoother surfaces produced tighter ejection profiles. This is promising, as it implies the particles will be ejected compactly and can be addressed with a single ultrafast pulse.

In order to replicate these results, we will use a Spectra-Physics Evolution-X pump beam, which is traditionally used to amplify an ultrafast pulse. It produces 527 nm light,

in pulses of up to $E = 10$ mJ and as short as $\tau = 10$ ns. With a nominal beam diameter of $D = 3$ mm, the maximum fluence is initially 140 mJ/cm^2, and the intensity is 14 MW/cm^2. This is the beam as it exits the laser cavity. Using a convex lens of focal length f, we can focus the radius of the beam down to some w_0 given by:

$$w_0 = \frac{f\lambda}{D\pi} \tag{11}$$

Because we want to be able to fine tune our spot size, we chose a long focusing lens with $f = 40$ cm. This gives a minimum beam diameter of 44.73μm. At this size the maximum fluence has increased to 630 J/cm^2, and the intensity can be as high as 63 MW/cm^2. Using a smaller focusing lens we could make the spot size even smaller and increase these values, but that should not be necessary. We are already achieving fluences many orders of magnitude larger than anything found in any laser cleaning paper. In order to accurately determine the size of the beam when it hits the substrate, a CCD camera is necessary. In the interest of time and because this is a proof of concept experiment, we would like to be able to approximate the position of best focus. From Gaussian optics, we know that once a beam reaches its minimum radius w_0 the distance over which is grows to a size of $w_0\sqrt{2}$ is called the "Rayleigh length", z_r.

$$z_r = \frac{\pi w_0^2}{\lambda} \tag{12}$$

For our beam and a 40 cm focusing lens, this comes out to 3.0 mm. Therefore, we have a ± 3 mm margin of error over which we can place our sample and still receive at least one half of the maximum possible fluence. This is an acceptable error.

The theory of dry laser cleaning is as follows. Consider a laser pulse of fluence F normally incident on a substrate. Let the substrate have reflectivity R, density ρ and specific heat C, and the laser penetrate to a thermal diffusion length μ. According to [16] we can equate the energy absorbed to a change in temperature ΔT and find

$$\rho C \Delta T = \frac{(1-R)F}{\mu} \tag{13}$$

Let this change in temperature cause a linear expansion of the surface, H. Assuming H is small:

$$H = \alpha \mu \Delta T \tag{14}$$

Where α is the coefficient of thermal expansion. Combining these two equations we get a final expression for the expansion

$$H = \frac{(1-R)F\alpha}{\rho C} \tag{15}$$

This implies that in order to make the most of the method, we want a substrate with high absorbance. On the other hand, we do not want the particles to absorb any radiation. This would cause them to thermally expand and warp, but we want the ultrafast pulse to interact with perfect spheres. Glass and ITO slides are ruled out as substrates because they are transparent, but silicon is very absorbing in the visible band. A 600 μm plate of silicon will reflect 37.6% of incident 525 nm light and absorb the rest.[21] In addition to the fact that silicon images very well under an SEM, this makes it the obvious choice for a substrate. As for the particle, the results of Zapka & Ziemlich rule out gold- it will melt under the laser pulse. Polystyrene, on the other hand, has an absorption coefficient of essentially 0 at this wavelength.[22] Therefore, we will take a diluted solution of polystyrene spheres in ethanol and drop it onto silicon wafers.

The first task is to show that dry laser cleaning is actually possible, and determine what power to set the laser at. More power should remove more spheres, but also result in worse damage to the substrate. At a certain point we may begin ablating the silicon, sending debris into the air along with the nanoparticles. This would make our ejection worthless. We diluted 500 nm polystyrene spheres at a ratio of 1000:1, and put a single drop on a 1 cm^2 silicon slide. The spheres dried very unevenly. Figure 6 displays SEM pictures of two portions of the slide at 1000x magnification. On one part of the slide we see ideal, disperse, barely clumped coverage. On the other the spheres are highly clumped and layered, making them difficult to image. In the middle of this image there is a spot of missing spheres, from where we pulsed the laser with 0.19 mJ. This was the lowest energy for which we observed particle removal. From this picture I estimate the diameter of our beam to be about 55μm. Therefore, the fluence delivered was about 8J/cm^2.

The more energy we put into the pulsed beam, the larger the cleared area was in general. This implies the impact is sending out a shockwave, removing spheres far outside the immediate impact area. This is promising, as spheres ejected in this fashion can not have been melted or otherwise damaged by the laser. For our most powerful shot (2.88 mJ, 121 J/cm^2), the cleaned area had a diameter of around 400 μm. While heavily covered areas (such as in figure 7(a)) tended to be thoroughly cleaned, we were not so successful in the less sparsely populated areas. Additionally, we found that the cleaning tended to be most striking far away from the impact site, and there would be a hard boundary between where the spheres were removed and where they remained. This is counter-intuitive, and we have no explanation for why it might be occurring. Finally, at higher energies we observed significant damage to the silicon. This zone of significant damage was as large as 200 μm for the highest energy shots. The lowest energy that produced noticeable damage was 1.38 mJ, corresponding to 58 J/cm^2, although invisible damage was probably occurring at lower fluences. Some representative images are shown in figure 7. At the lowest energies there is no sphere removal or substrate damage. At the highest energy there are thousands of spheres removed over a large area, and massive damage is done to the substrate. We have a very high degree of control between these two extremes.

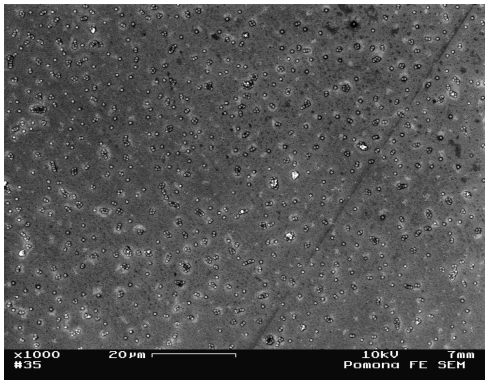

(a) This is the type of monodisperse, non-clumped sphere coverage we hope to achieve. There are some isolated large clumps, but they are generally not a problem. From this image I estimate the sphere coverage (excluding the enormous clumps) to be on the order of 100,000 spheres per mm^2.

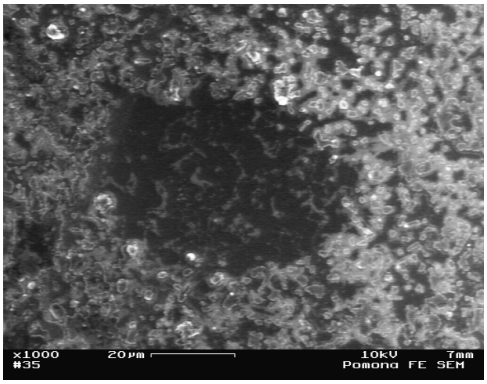

(b) In this picture the spheres are much more clumped and layered above each other, making them difficult to image. The spot in the center is the result of a 0.19 mJ laser pulse: the lowest energy pulse for which we observed sphere removal. Based on this spot, I estimate the size of our laser beam at impact to be around 55 μm. I will use this size to estimate the fluence in subsequent shots.

FIGURE 6. Two SEM images of a silicon slide with one drop of 1:1000 500nm polystyrene spheres to ethanol deposited and allowed to dry. As you can see, the resulting density is far from uniform. Figure (a) also shows the results of a low power laser shot.

8. Conclusions

Despite their theoretical promise, electrostatic and mechanical ejection both proved fruitless. In the field of fine particle adhesion, it is widely believed that Van der Waals forces dominate on the micro and nano scale, but we have come to believe this is not the case. The only thing that can explain the tenacity of these spheres is a persistent meniscus, caused by crystallization around impurities in the solution.

Laser cleaning, however, has been demonstrated to removed 500 nm spheres very effectively. The work done by Lu et. al. implies that most of the spheres are ejected directly back along the incident laser beam, making this a promising device for studying ultrafast non-linear phenomena in wavelength scale particles. In order to make this a completely functional method, the speed and profile of the ejected particles must be characterized. Our current plan is to pass a continuous laser beam parallel to the substrate and observe the ensuing Mie scattering off the ejected particles. Work has already begun in this endeavor, and will continue into the next semester.

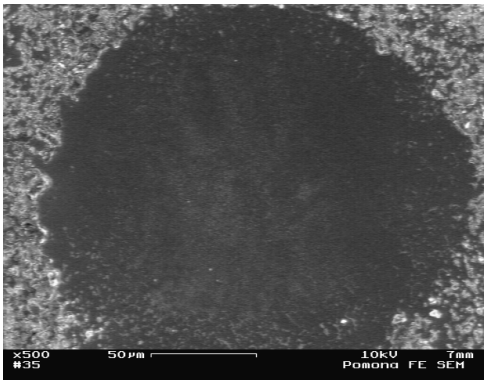

(a) A pulse with 0.41 mJ, or 17 J/cm^2. The cleaned area has a diameter of roughly 200 μm, and substrate damage is low or non-existent (the white streaks in the center may or may not be a result of the laser). The cleaning is total at the center of the beam and less effective around the edges, as expected.

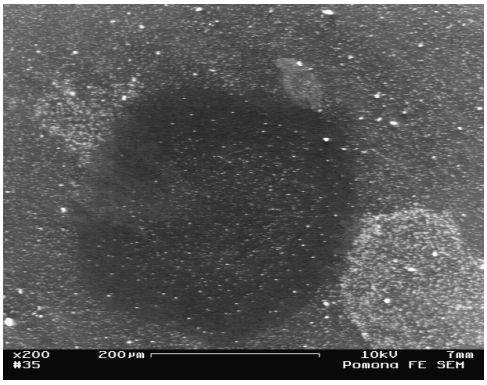

(b) A pulse with 1.17 mJ, or 49 J/cm^2. The spot size has grown to about 300 μm, yet the cleaning is not as efficient, despite this pulse having more energy than the one in figure(a). We repeatedly observed that less thoroughly covered areas did not clean as well, and we do not know why. The cleaning is least efficient right as the center, but there is an outer annulus in which all the spheres were removed. We do not know why this is.

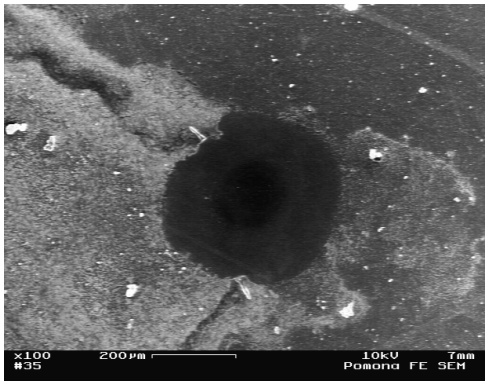

(c) A pulse with 2.72 mJ, or 115 J/cm^2. The cleaning is nearly total over a 400 μm spot size, and there is a 150 μm spot on which the substrate is heavily damaged.

FIGURE 7. A silicon wafer was coated in 500nm polystyrene spheres and pulsed once each at 33 locations with energies ranging from 0.01 mJ to 2.88 mJ. The results of three of these pulses are shown above; this is meant to be representative of the wide range of behavior observed.

References

[1] Sumeruk H.A. et. al., *Control of Strong-Laser-Field Coupling to Electrons in Solid Targets with Wavelength-Scale Spheres* Phys. Rev. Lett. 98 (4), 045001 (2007).

[2] Breizman B.N., Arefiev A.V., Fomyts'kyi M.V., *Nonlinear physics of laser-irradiated microclusters* Phys. Plas. 12, 056706 (2005).

[3] Higginbotham A. P. et. al. *Generation of Mie size microdroplet aerosols with applications in laser-driven fusion experiments* Review of Scientific Instruments 80 (6), 063503 (2009).

[4] Badger, Marc *Improving Targets for Laser Fusion Experiments: Developing an Electrostatic Delivery Device* Senior Thesis, Harvey Mudd College, (2010).

[5] Moore, John & David, Christopher & Coplan, Michael. *Building Scientif Apparatus.* Cambridge University Press, New York, 4th edition, 2009. 93-131.

[6] Castellanos A., *The relationship between attractive interparticle forces and bulk behavior in dry and uncharged fine powders* Advances in Physics 54 (4), 263 (2005).

[7] Takeuchi M., *Adhesion forces of charged particles* Chemical Engineering Science 61, 2279 (2006).

[8] Murata Manufacturing Co., Ltd. *Piezoelectric Ceramics (PIEZOTITE) Sensors.* Catalogue No. P19E-9

[9] Princen H. M., *The Equilibrium Shape of Interfaces, Drops, and Bubbles. Rigid and Deformable particles at interfaces* Surface and Colloid Science 2, 22-29. Ed. Marijevic E., Borkovec, M.

[10] Cross N. L., Picknett R. G., *The Liquid Layer between a Sphere and a Plane Surface* Transactions of the Faraday Society 59, 846 (1962).

[11] Ranade M. B., *Adhesion and Removal of Fine Particles on Surfaces* Aerosol Science and Technology 7, 161 (1987).

[12] Wright, Ian, *Generation of Nanoparticles via Atomization of Chitosan Solutions using Piezoelectric Oscillators* Senior Thesis, Harvey Mudd College (2009).

[13] Hecht L., *An Introductory Review of Particle Adhesion to Solid Surfaces* Journal of the IES 33, 33 (1990).

[14] Zapka W., Ziemlich W., Tam A. C., *Efficient pulsed laser removal of 0.2um sized particles from a solid surface* Appl. Phys. Lett. 58 (20), 2217 (1991).

[15] Imen K., Lee S. J., Allen S. D., *Laser-assisted micron scale particle removal* App. Phys. Lett. 58 (2), 203 (1990).

[16] Tam A. C., Leung W. P., Zapka W., Ziemlich W., *Laser-cleaning techniques for removal of surface particulates* J. Appl. Phys. 71 (7), 3515 (1992).

[17] Lee S. J., Imen K., Allen S. D., *Laser-assisted particle removal from silicon surfaces* Microelectronic Engineering 20, 145 (1993).

[18] Lu Y. F., Song W. D., Hong M. H., Teo B. S., Chong T. C., Low T. S., *Laser removal of particles from magnetic head sliders* J. App. Phys. 80 (1), 499 (1996).

[19] Lu Y. F., Zheng Y. W., Song W. D., *Laser induced removal of spherical particles from silicon wafers* J. App. Phys. 87 (3), 1534 (2000).

[20] Lu Y. F., Zheng Y. W., Song W. D., *Characterization of ejected particles during laser cleaning* J. App. Phys. 87 (1), 549 (2000).

[21] Virginia Semiconductor, Inc., *Optical Properties of Silicon* Web. http://www.virginiasemi.com/pdf/Optical Properties of Silicon71502.pdf. 21 July 2010.

[22] Jain P. K., Lee K. S., El-Sayed I. H., El-Sayad M. A., *Calculated Absorption and Scattering Properties of Gold Nanoparticles of Different Size, Shape, and Composition: Applications in Biological Imaging and Biomedicine* J. Phys. Chem. B 110, 7238 (2006).